Surface & Coatings Technology xxx (2009) xxx–xxx

Contents lists available at ScienceDirect

Surface & Coatings Technology

journal homepage: www.elsevier.com/locate/surfcoat

Water adsorption on phosphorous-carbide thin films

E. Broitman [a,*], A. Furlan [b], G.K. Gueorguiev [b], Zs. Czigány [c], A.M. Tarditi [d], A.J. Gellman [a], S. Stafström [b], L. Hultman [b]

[a] Carnegie Mellon University, 5000 Forbes Avenue, Rook DH-1208, Pittsburgh, PA 15213, USA
[b] Linköping University, SE 58183 Linköping, Sweden
[c] Research Institute for Technical Physics and Materials Science, 1525 Budapest, Hungary
[d] Universidad Nacional del Litoral, 3000 Santa Fe, Argentina

ARTICLE INFO

Available online xxxx

Keywords:
Phosphorous carbide
Dangling bonds
Water adsorption
Density functional theory

ABSTRACT

Amorphous phosphorous-carbide films have been considered as a new tribological coating material with unique electrical properties. However, such CP_x films have not found practical use until now because they tend to oxidize/hydrolyze rapidly when in contact with air. Recently, we demonstrated that CP_x thin films with a fullerene-like structure can be deposited by magnetron sputtering, whereby the structural incorporation of P atoms induces the formation of strongly bent and inter-linked graphene planes. Here, we compare the uptake of water in fullerene-like phosphorous-carbide (FL-CP_x) thin films with that in amorphous phosphorous-carbide (a-CP_x), and amorphous carbon (a-C) thin films. Films of each material were deposited on quartz crystal substrates by reactive DC magnetron sputtering to a thickness in the range 100–300 nm. The film microstructure was characterized by X-ray photoelectron spectroscopy, and high resolution transmission electron microscopy. A quartz crystal microbalance placed in a vacuum chamber was used to measure their water adsorption. Measurements indicate that FL-CP_x films adsorbed less water than the a-CP_x and a-C ones. To provide additional insight into the atomic structure of defects in the FL-CP_x and a-CP_x compounds, we performed first-principles calculations within the framework of density functional theory. Cohesive energy comparison reveals that the energy cost formation for dangling bonds in different configurations is considerably higher in FL-CP_x than for the amorphous films. Thus, the modeling confirms the experimental results that dangling bonds are less likely in FL-CP_x than in a-CP_x and a-C films.

1. Introduction

Amorphous carbon-based thin films are used in many tribological applications as protective coatings and solid lubricants. By tuning the C sp^3-to-sp^2 bonding ratio and by alloying the carbon with other elements, like H, N, Si, F, W, etc, the properties of the coatings can be tailored [1]. Recently, we have shown that it is possible to incorporate fullerene-like features to a solid matrix of C and N. The resulting so called fullerene-like (FL) compound consists of sp^2-coordinated graphitic basal planes that are buckled due to the presence of pentagons and cross-linked at sp^3-hybridized C sites, both of which are caused by structural incorporation of nitrogen. This fullerene-like carbon nitride (FL-CN_x) has many tribological advantages over amorphous carbon nitride (a-CN_x) in properties such as hardness, friction coefficient, wear resistance, and elastic recovery [2–5].

Phosphorous can be viewed as an alternative dopant to N. Amorphous phosphorous-carbide (a-CP_x) films, studied primarily for his peculiar electrical properties [6,7] have recently been shown as a potential new tribological coating material [8,9]. Previously synthesized phosphorous-carbide films, most of them with high P content, have shown an amorphous structure. Typical for such films is a hydrogen content reaching 10% and their liability to oxidation [10,11]. Recently, we demonstrated that CP_x thin solid films with a fullerene-like structure can be deposited by magnetron sputtering. Thus, the introduction of P atoms in the graphene structure induces the formation of strongly bent and inter-linked graphene planes [8,12,13].

The largest industrial application of carbon-nitride films is in the magnetic storage devices. These carbon-based coatings are amorphous, containing hydrogen to saturate the dangling carbon bonds and nitrogen to improve the overcoat durability. In a previous work we compared the uptake of water of these commercial coatings with a-C, a-CN_x and FL-CN_x films and found that, due to lower water adsorption, the fullerene-like coatings have a potential application in the hard disk industry [14,15].

In this work we compare the uptake of water of amorphous phosphorous-carbide films (a-CP_x), with fullerene-like phosphorous-carbide (FL-CP_x) and amorphous carbon films. Films with thickness in the range 100–300 nm were deposited on quartz crystal substrates by

* Corresponding author. Department of Chemical Engineering, Carnegie Mellon University, 5000 Forbes Avenue, Rook DH-1208, Pittsburgh, PA 15213, USA. Tel.: +1 412 268 9537; fax: +1 412 268 7139.
E-mail address: broitman@andrew.cmu.edu (E. Broitman).

0257-8972/$ – see front matter © 2009 Elsevier B.V. All rights reserved.
doi:10.1016/j.surfcoat.2009.06.003

reactive DC magnetron sputtering. The film microstructure was characterized by X-ray photoelectron spectroscopy, and high resolution transmission electron microscopy. A quartz crystal microbalance (QCM) placed in a vacuum chamber was used to measure their water adsorption.

To provide additional insight into the atomic structure of defects in phosphorous-carbide compounds, we performed first-principles calculations within the framework of density functional theory (DFT). We employed a similar simulation approach as the one used before on carbon nitrides [15] in order to provide additional insight on the energetics of dangling bonds in FL-CP_x, a-CP_x and a-C compounds.

2. Experimental details

The CP_x films were deposited onto quartz substrates by DC magnetron sputtering from a compound target containing carbon and 12 at.% of P at two different substrate temperatures (T_s), as described previously [16,17]. The high-vacuum system had a base pressure of $\sim 5\times10^{-7}$ Torr. The magnetron was operated in an Ar discharge with a gas pressure (P_{Ar}) at 3 mTorr, 250 W of applied power, and a bias voltage (U_b) of −25 V was applied while T_s was varied between 150 and 300 °C. The a-C films were deposited from a pure C target at $P_{Ar}=3$ mTorr, $T_s=150$ °C, 250 W of applied power, and $U_b=-25$ V. The films were deposited onto both sides of quartz crystals with thickness of ~100–300 nm, at a deposition rate of ~0.04 nm/s.

The apparatus designed and constructed for measurement of humidity adsorption has been described previously [14,18]. It consists of a vacuum chamber that can be evacuated by a turbopump or a sorption pump and operates in the range 10^{-8}–10^{3} Torr. A capacitance manometer was used to measure the partial pressure of water in the range 10^{-1}–10^{3} Torr. The QCM housing is capable of holding 3 quartz crystals for simultaneously monitoring water adsorption on three surfaces. The temperature of the QCM, measured by a thermocouple, is controlled at 50 °C to allow a stable measurement [14]. The mass of water adsorbed on the surface of the quartz crystal was calculated using the Sauerbrey equation $\Delta f=-C\Delta m$, where Δf and Δm are the change of frequency and the adsorbed mass of water, respectively, and C depends on the physical properties of the quartz crystal [14].

The P bonding of the films was investigated by X-ray photoelectron spectroscopy (XPS) using a VG Scientific MICROLAB 310-F system and the microstructure of the films was examined with a Technai G2 operated at 200 kV for high resolution transmission electron microscopy (HR-TEM) [17].

3. Computational details

Finite model systems simulating a-C, a-CP_x, as well as systems in which P is incorporated in strongly interlocked graphene sheets (to represent FL-CP_x) were considered. The study involved both geometry optimizations and cohesive energy (E_{coh}) calculations performed within the DFT framework in its Generalized Gradient Approximation (GGA). Differences in cohesive energies $|\Delta E_{coh}|$ for the possible structures are determined by an optimization strategy presented elsewhere [19], making use of the Gaussian 03 program [20]. For the DFT-GGA, the Perdew–Wang exchange-correlation functional (PW91) [21] and the B3LYP hybrid functional [22] were used. Both are known to provide an accurate description of the structural and electronic properties of FL thin films [19] and similar covalent systems [23–25]. For both carbon and phosphorus, double-ζ basis sets augmented with polarization functions were used. The results reported in this work correspond to PW91 exchange-correlation functional while B3LYP simulations were reserved for test purposes.

4. Results and discussion

4.1. Film composition and structure

Deposition experiments were performed at different substrate temperatures in order to synthesize FL-CP_x and a-CP_x films. The quantitative analysis of the XPS signal has revealed CP_x films deposited at 150 °C have $x=0.24$ and the ones deposited at 300 °C have $x=0.1$. The analysis of the P*2p* photoelectrons confirmed the presence of a peak at approximately 130 eV, identified as a P–C bonding [17]. High resolution transmission electron microscopy has shown that CP_x films grown at 300 °C (Fig. 1a) exhibit short-range ordering with fragments of curved graphene sheets, characteristic of a fullerene-like structure. In contrast, CP_x films deposited at 150 °C (Fig. 1b) show an amorphous structure. Cross-sectional scanning electron microscopy has shown a dense CP_x film structure without voids or columnar structure [9]. On the other hand, a-C films exhibit a porous structure [1].

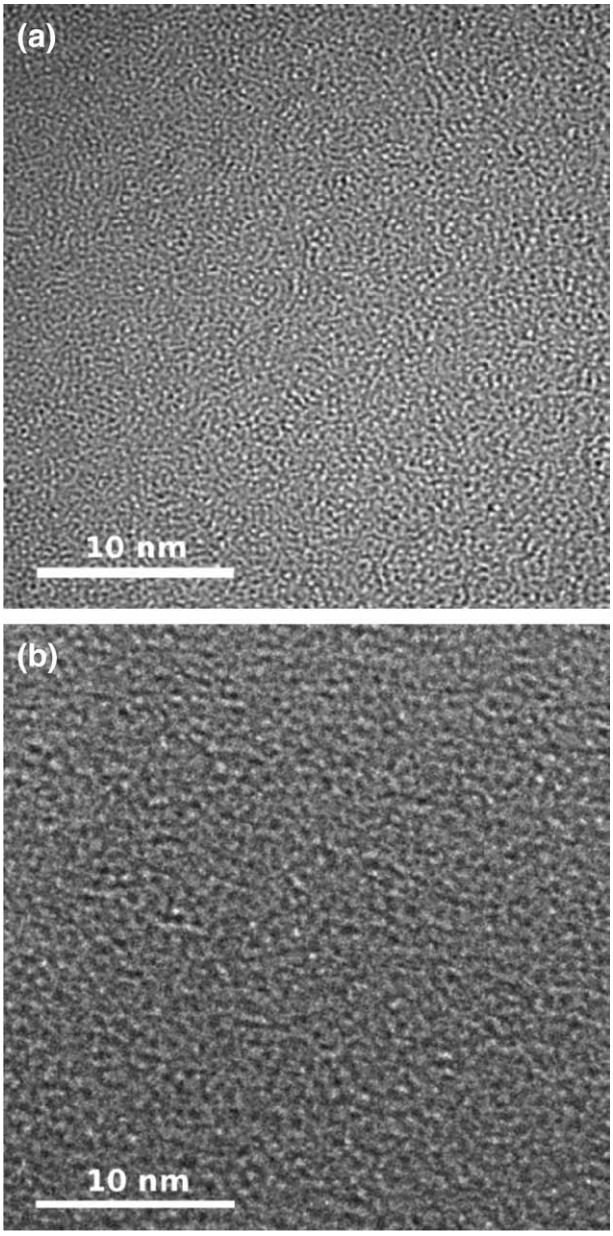

Fig. 1. HR-TEM of CP_x thin films deposited at different substrate temperatures a) $T_s=300$ °C (fullerene-like structure); b) $T_s=150$ °C (amorphous structure).

Please cite this article as: E. Broitman, et al., Surf. Coat. Technol. (2009), doi:10.1016/j.surfcoat.2009.06.003

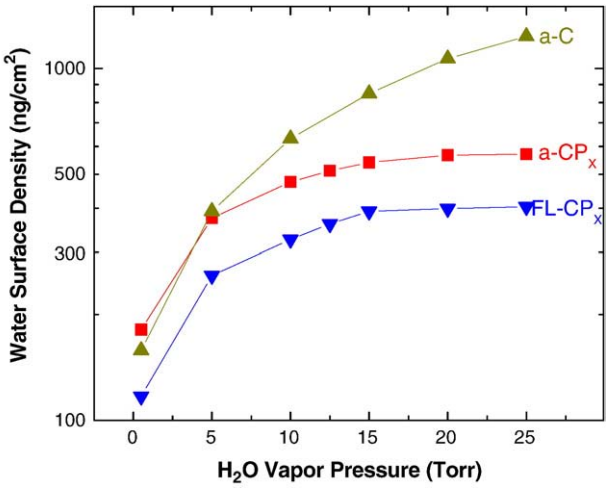

Fig. 2. The water surface density adsorbed on the surface of quartz crystal with carbon overcoats at 50 °C versus water vapor pressure. The density was calculated as the total adsorbed mass Δm divided by the surface area of the crystal.

4.2. Adsorption of H_2O on CP_x overcoats

Fig. 2 shows the adsorption of water versus the water vapor pressure for films deposited under different conditions. All carbon-based films have a characteristic dependence of water coverage on the H_2O vapor pressure. There are, however, differences in the amounts of the adsorbed water:

i) Pure carbon films adsorb more water than phosphorous-carbide films;
ii) Fullerene films adsorb less water than amorphous films.

There are very few comparative studies on the adsorption of water on carbon films with different microstructure and/or composition [14]. Smallen et al. [26] investigated the water adsorption of CH_y films deposited by sputtering in different Ar-C_2H_2 gas mixtures (0–30% of C_2H_2). Their ellipsometric measurements of the thickness of adsorbed water have shown that the adsorption increased with the relative humidity (RH) and concentration of hydrogen in the film. Lee [27] studied indirectly the adsorption of water on a-CN_x films. He measured the electrical properties of the coatings as a function of ambient humidity, and proposed the a-CN_x film as a novel humidity sensor. In a previous work, we have compared the water adsorption of a-C, a-CN_x and FL-CN_x films [28]. We reported that FL-CN_x shows the lower adsorption rate, and that a-C adsorbs more than 14 times the amount adsorbed by the fullerene coatings [14].

It has been shown the surface roughness could play an important role on the water adsorption [26]. We have reported previously that the a-C films have an rms roughness of 15 nm, the a-CP_x has 0.9 nm, while FL-CP_x has the lowest roughness (0.5 nm) [1,3]. The surface roughness seems to correlate well with the water adsorption behavior shown in Fig. 2. However, surface roughness differences are small in our case, and only play a role in the adsorption of water at high levels of RH, where capillary condensation can occur in the valleys giving thicker water films [14].

The surface of the sputtered carbon-based films is heterogeneous and is composed of different hybridized carbon atoms (sp, sp^2, and sp^3) and dangling bonds. As soon as the surface is exposed to air, its dangling bonds react with oxygen and form oxygen containing polar groups such as C–O–C, C–OH, and C=O [29,30]. Because of the hydrogen bonding tendency of water, the adsorption of water is sensitive to the polarity of the adsorbent surface [26] and is enhanced by the presence of oxidized carbon. We should expect that, because of the fullerene structure, FL-CP_x films have the lowest number of dangling bonds and, in consequence, low water adsorption. Electron spin resonance measurements confirmed this assumption for carbon-nitride coatings [15]. The differences in adsorption on our films must be understood in the context of their microstructural differences, as explained in the next section by a theoretical model.

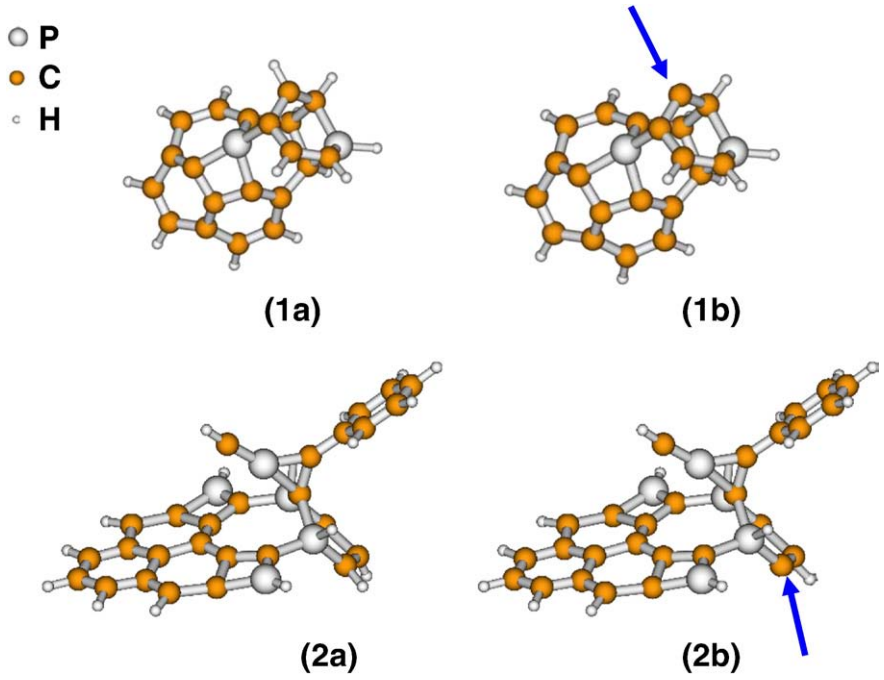

Fig. 3. FL-CP_x model systems: In the first row the model system 1 is a stable cage-like structure: (1a) configuration without dangling bonds; (1b) system with a dangling bond. In the second row the system 2 corresponds to inter-linked model system containing tetragons and: (2a) without dangling bonds; (2b) with a dangling bond. In figures (1b) and (2b) the arrows indicate the location of the dangling bonds.

Please cite this article as: E. Broitman, et al., Surf. Coat. Technol. (2009), doi:10.1016/j.surfcoat.2009.06.003

Table 1
PW91 cohesive energies E_{coh} corresponding to the model systems displayed in Figs. 3 and 4.

		a (no dangling bonds)	b (with a dangling bond)
FL-CP_x model system 1	E_{coh} (eV)	5.29	4.24
	ΔE_{coh} (eV)	0	1.04
FL-CP_x model system 2	E_{coh} (eV)	6.37	5.75
	ΔE_{coh} (eV)	0	0.62
a-CP_x	E_{coh} (eV)	11.19	10.64
	ΔE_{coh} (eV)	0	0.55
a-C	E_{coh} (eV)	12.45	11.98
	ΔE_{coh} (eV)	0	0.47

$\Delta E_{coh} = E_{coh}$ (model system with a dangling bond) $- E_{coh}$ (analogous model system *but* without dangling bonds).

4.3. Theoretical modeling

4.3.1. Energy cost for defects as a measure for occurrence of dangling bonds in FL-CP_x

Different model systems containing pentagons, tetragon defects, strongly interlocked graphene sheets and cage-like formations have been shown to correctly describe FL-CP_x [19]. Both a-CP_x and a-C were simulated by optimizing structurally disturbed model systems consisting on randomly intersected P-containing and pure graphene sheets, respectively. As a result of the optimization procedure both a-CP_x and a-C exhibit a mixture of sp^3 and to a lesser extent sp^2 bonding types which is considered the correct model for a-C. In the present work, by considering typical FL-CP_x, a-CP_x and a-C model systems, we specifically focus our attention on the cohesive energy cost for formation of defects associated with dangling bonds.

Fig. 3 displays FL-CP_x model systems employed in the simulations of the present work. Fig. 3(1a) and (1b) show a stable cage-like FL-CP_x structure ($C_{20}P_2H_{13}$) and its counterpart containing a dangling bond, respectively. Fig. 3(2a) and (2b) display a prototypical for FL-CP_x inter-linked model system containing tetragons ($C_{27}P_5H_{18}$) and its counterpart containing a dangling bond, respectively.

In FL-CN_x and a-CN_x compounds, the dangling bonds are frequently localized at the sites where pyridine-like defects happen [15]. However, for FL-CP_x and a-CP_x thin films, pyridine-like defects are not an issue due to the differences in chemical bonding which nitrogen and phosphorus form with carbon. As a result, in CP_x compounds the diversity of dangling bonds is not as obvious as in CN_x but, nonetheless, it exits and depends on factors such as how close to a P-site is located a given dangling bond, whether a dangling bond occurs at a tetragon, a pentagon, a cross-linking between graphene planes, etc.

The cohesive energy E_{coh} of a model system is defined as the energy required for breaking the system into isolated atomic species, i.e.,

$$E_{coh} = E_{total} - \sum_i E_{i,total}^{isolated}. \quad (1)$$

i stands for different constituent atoms. In Table 1 the PW91 E_{coh} for the structures displayed in Figs. 3 and 4 are listed. ΔE_{coh} stays for the energy cost for dangling bonds formation with reference to the analogous structures but without dangling bonds.

The energy costs for formation of a dangling bond at different sites in the cage-like system shown in Fig. 3(1a) and the inter-linked configuration displayed in Fig. 3(2a) were compared. The results listed in Table 1 correspond to the lowest energy cost for formation of a dangling bond in the considered model systems. Fig. 3(1b) and (2b) indicate the sites at which these energetically most favorable dangling bonds occur.

The energy cost for formation of a dangling bond is by ~0.3 eV higher for the cage-like FL-CP_x (Fig. 3, first row) than for the inter-linked FL-CP_x structure (Fig. 3, second row). While the first row systems in Fig. 3 can be seen as simulating more ordered FL-CP_x, which works as a seed for onion-like structural features in FL-CP_x as shown in Ref. [12], the inter-linked system in the second row in Fig. 3 illustrates a structural element invoking more disordered and interlocked phosphorus carbide. Thus, the cohesive energy data presented in Table 1 suggests that the occurrence of dangling bonds is less frequent in FL-CP_x compounds with more ordered structure; they correspond to lower phosphorus content ($\leq$15 at.%) for which more onion-like structural features and lower density of inter-linkages is expected [19].

The energy differences ΔE_{coh} considered in the present evaluation of energy cost for formation of dangling bonds are several times larger than the thermal energy at growth environment temperatures (~0.065 eV). Consequently, ΔE_{coh} appears as an appropriate criterion

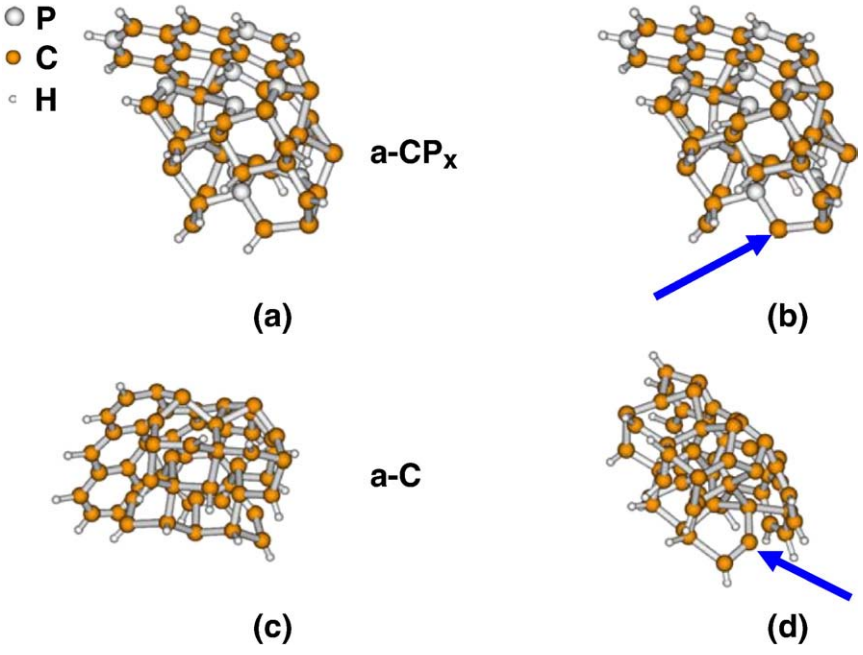

Fig. 4. a-CP_x (top row) and a-C (bottom row) model systems: (a) without a dangling bond; (b) with a dangling bond (the arrows point to the location of the dangling bond).

Please cite this article as: E. Broitman, et al., Surf. Coat. Technol. (2009), doi:10.1016/j.surfcoat.2009.06.003

for likeliness of structural features in carbon-based compounds grown at such conditions.

4.3.2. Energy cost for dangling bonds in a-CP_x and a-C

The lower energy cost for dangling bonds in CP_x systems containing interlocked graphene sheets suggests that higher occurrence of dangling bonds can be expected when CP_x compounds get gradually less ordered (or more amorphous). Such material can be seen as a structural transition between FL-CP_x and a-CP_x.

To compare the cost for dangling bonds in a-CP_x and a-C to the data reported above for FL-CP_x, we optimize model systems representing amorphous compounds which contain a mixture of sp^2/sp^3-coordinated networks. Fig. 4(a) and (b) show typical a-CP_x structures without and with a dangling bond, respectively. In both cases the structures have the lowest possible energy cost for the given structure. As seen from Table 1, in a-CP_x the energy cost for formation of a dangling bond is 0.55 eV (to be compared to 0.62–1.04 eV for FL-CP_x). i.e., higher density of dangling bonds is expected in a-CP_x solid material.

Fig. 4(c) and (d) display structures corresponding to pure a-C without and with a dangling bond, respectively. A typical model system representing a-C consists of randomly interconnected pieces of graphene sheets which after relaxation evolve to a mixed mostly sp^2/sp^3-coordinated C network. In a-C the energy cost for a dangling bond reads 0.47 eV which is lower than in a-CP_x and by ~0.15–0.6 eV lower than in FL-CP_x (see Table 1). Thus, in a-C, the likeliness of dangling bonds is considerably higher than in FL-CP_x, and still to some extent higher than in a-CP_x.

5. Conclusions

QCM measurements have probed the effect of microstructure and composition of carbon-based thin films intended for overcoats on the adsorption of water. The results indicate the microstructure of the films influences the adsorption level: amorphous films absorb significantly more water than the nanostructured FL-CP_x films. Our results suggests the lower water adsorption on FL-CP_x films correlates with a decrease of dangling bonds on the film surface, as in the case of CN_x compounds.

First-principles calculations reveal that the energy cost for dangling bonds in different configurations is considerably higher in FL-CP_x than for amorphous films, being the lowest in pure a-C. Thus, our simulations confirm the experimental results that dangling bonds are less likely in FL-CP_x than in a-CP_x and a-C films. The water adsorption of fullerene-like phosphorous-carbide films is lower than on a-CP_x and a-C films. Taking into consideration their electrical and tribological properties, FL-CP_x overcoats have a potential application in the hard disk industry.

Acknowledgments

E.B. and A.G. acknowledge the Data Storage Systems Center from Carnegie Mellon University. G.K.G. acknowledges The Swedish Research Council and the European Commission under the project FOREMOST. A.F. and L.H. acknowledge The Swedish Foundation for Strategic Research (SSF).

References

[1] E. Broitman, J. Neidhardt, L. Hultman, in: C. Donnet, A. Erdemir (Eds.), Tribology of Diamond-Like Carbon Films: Fundamentals and Applications, Springer, N. York, 2007, p. 620.
[2] E. Broitman, et al., Wear 248 (1–2) (2001) 55.
[3] J. Neidhardt, et al., Diam. Relat. Mater. 13 (10) (2004) 1882.
[4] E. Broitman, et al., Diam. Relat. Mater. 9 (12) (2000) 1984.
[5] E. Broitman, et al., Appl. Phys. Lett. 72 (20) (1998) 2532.
[6] S.M. Mominuzzaman, et al., Diam. Relat. Mater. 10 (9–10) (2001) 1839.
[7] A. Liu, et al., Phosphorus Sulfur Silicon Relat. Elem. 183 (2) (2008) 657.
[8] A. Furlan, et al., Physica Status Solidi (RRL) — Rapid Res. Lett. 2 (4) (2008) 191.
[9] Furlan, A., et al., Structure and properties of phosphorous-carbide thin solid films. Unpublished.
[10] S.R.J. Pearce, et al., Diam. Relat. Mater. 11 (3–6) (2002) 1041.
[11] F. Claeyssens, et al., Appl. Phys., A Mater. Sci. Process. 79 (4) (2004) 1237.
[12] G.K. Gueorguiev, et al., Chem. Phys. Lett. 426 (4–6) (2006) 374.
[13] A. Furlan, et al., Thin Solid Films 515 (3) (2006) 1028.
[14] E. Broitman, et al., Thin Solid Films 513 (3) (2006) 979.
[15] E. Broitman, et al., Thin Solid Films 517 (3) (2008) 1106.
[16] A. Furlan, et al., Structure and properties of phosphorous-carbide thin solid films. Submitted, 2009.
[17] A. Furlan, et al., Phys. Status Solidi (RRL) — Rapid Res. Lett. 2 (4) (2008) 191.
[18] E.B. Svedberg, N. Shukla, Tribol. Lett. 17 (4) (2004) 947.
[19] G.K. Gueorguiev, et al., Chem. Phys. Lett. 410 (4–6) (2005) 228.
[20] M.J. Frisch, Gaussian, Inc., Wallingford, CT, 2003.
[21] J.P. Perdew, et al., Phys. Rev. B 46 (11) (1992) 6671.
[22] A.D. Becke, J. Chem. Phys. 98 (7) (1993) 5648.
[23] S. Stafstrom, L. Hultman, N. Hellgren, Chem. Phys. Lett. 340 (3–4) (2001) 227.
[24] R.H. Xie, et al., J. Chem. Phys. 118 (19) (2003) 8621.
[25] R.H. Xie, G.W. Bryant, V.H. Smith, Chem. Phys. Lett. 368 (3–4) (2003) 486.
[26] M. Smallen, et al., IEEE Trans. Magn. (1994) 4137.
[27] G.L. Lee, S.L. Lee, Sens. Actuators B 108 (2005) 450.
[28] E. Broitman, et al., J. Electron. Mater. 31 (9) (2002) L11.
[29] N. Shukla, A.J. Gellman, J. Gui, Langmuir 16 (16) (2000) 6562.
[30] R.H. Wang, et al., IEEE Trans. Magn. 32 (5) (1996) 3777.

Please cite this article as: E. Broitman, et al., Surf. Coat. Technol. (2009), doi:10.1016/j.surfcoat.2009.06.003